Magazine of Civil Engineering

ISSN 2712-8172

journal homepage: http://engstroy.spbstu.ru/

Research article

UDC 626/627:699.841:624.1

DOI: 10.34910/MCE.121.2

Soil friction on a retaining wall under seismic load

O.P. Minaev [1,2] ✉

[1] *Military Academy of Logistics named after General of the Army A.V. Hrulev, St. Petersburg, Russian Federation*

[2] *Admiral Makarov State University of Maritime and Inland Shipping, St. Petersburg, Russia Federation*

✉ *minaev.op@bk.ru*

Keywords: retaining wall, active pressure, soil friction, dynamic load, foundation, bearing capacity, stability, wave action, seismic intensity

Abstract. The paper is the first to establish that the classical quasi-static analytical calculation of the retaining wall for seismic load indirectly reflects the wave nature of the impact of the sandy backfill soil on the rear surface of a retaining wall. The evidence provided includes the comparative results of the designed gravity retaining wall made from reinforced concrete and having a front cantilever that consider and disregard soil friction under the calculated operational static and seismic loads. The calculations were carried out for given dimensions of the retaining wall and characteristics of sandy backfill soils on weak clay foundation soils. It is emphasized that the calculation results are quite consistent with the research data on the behavior of sandy soils in the plate base under dynamic wave loads. These results were used to obtain the dependence necessary for determining the angle of soil friction against the rear surface of the wall under seismic load of varying intensities. It seems quite convincing that the calculation of the retaining stack for a seismic load of 9 points can be carried out without taking into account soil friction, since in this case, under seismic action, soil slippage along the rear surface of the retaining wall is possible. With a seismic load of 7 and 8 (or less) points, the angle of friction of the soil against the rear surface of the retaining wall should be determined from the obtained dependence to determine the angle of friction of the soil under a seismic load of varying intensity given in this article.

Citation: Minaev, O.P. Soil friction on a retaining wall under seismic load. Magazine of Civil Engineering. 2023. 121(5). Article no. 12102. DOI: 10.34910/MCE.121.2

1. Introduction

The basic principles for calculating and designing the natural base and pile foundation of a gravity retaining wall for static (erection and operating) loads [1–8], as well as for dynamic one, in particular seismic load, have to be elaborated further and studied comprehensively considering the results of the calculation [1]. Modern geotechnical solutions that take into consideration static [9–12] and dynamic [13–19] loads are discussed in a number of works by Russian and foreign scientists.

Papers [20, 21] present the calculation results of different types of gravity retaining walls given a wide range of soil conditions in the foundation and sandy backfill soils for seismic load. However, these calculations do not consider the soil friction against the rear surface of the retaining wall.

It is known [1, 2] that the soil friction on the rear surface of the retaining wall significantly affects the results of the design carrying capacity and stability under static load of the retaining wall.

Usually (for example, [2]) calculations conventionally assume that the angle at which soil frictions against the retaining wall is equal to the angle φ of internal friction of the backfill soil or to its half $\varphi/2$.

Given the wave character of the dynamic effect on the retaining wall, it seems that such a convention in determining the angle of internal friction of soil against the retaining wall is not likely to be applicable to calculate seismic loads. The reason for that is described below.

Headed by Prof. P.L. Ivanov the soil mechanics laboratory of the Department of Underground Structures, Foundations and Bases, Peter the Great St. Petersburg Polytechnic University was responsible for numerous studies of the effect produced by dynamic wave load on the friction of sandy soil on the surface of a vibrating plate installed on its surface. In the experiments with a vibrating plate for in-plane shear, in addition to the static stresses from the weight of the plate and the vibrator, the mechanical vibrator added dynamic stresses from the rotation of the vibrator cams that acted according to harmonic law. The vertical mechanical vibrator varied the stresses raging within the values of $\pm\Delta\sigma$. The dynamic pressure amplitude was controlled by changing the eccentricity of the vibrator cams while the frequency was adjusted by their rotation speed. The shear resistance considered according to the Coulomb dependence in the form of $\tau = (\sigma - \Delta\sigma) tg\varphi$ indicates a periodic shear of the plate on the sand surface.

As a result of the tests it has been found that within the range of vibration acceleration up to 1.0 g the angle of internal soil friction does not change while the decreasing shear resistance should be taken into account through changing normal stresses at the plate bottom. Thus, in case of vibration and seismic effects the shear stability of structures has to be tested given the dynamic component of stresses at a constant value of the angle of internal soil friction, imposed on the static tests.

This work is aimed at identifying the calculation and design specifics of the natural base and pile foundation of a gravity reinforced concrete corner retaining wall with a front cantilever given seismic load. It also identifies the specific feature of the calculation and design of the natural base and pile foundation of a retaining wall considering the soil friction against the rear surface on the seismic load based on the results of the calculations obtained. In addition, we interpreted these results on the basis of the known research data on the behavioral patterns of sandy soils under dynamic loads and determined the dependence for calculating the angle of soil friction against the wall under seismic loads of various intensities.

In addition, we interpreted these results on the basis of known data from studies of the behavior of sandy soils under dynamic loads and obtained the dependence for calculating the angle of friction of the soil against the wall under seismic loads of various intensities.

2. Methods

2.1. Theoretical dependencies

When calculating static load, width b of the base of a reinforced concrete retaining wall with a front cantilever is usually determined using the formula of A.Z. Zarkhi, which has the following form

$$b = 2.2\sqrt{\frac{E_a y_a}{(h_w + h_{cant})(0.75\gamma_m - \gamma_w) + h_0\gamma_0}}, \quad (1)$$

where E_a is the active lateral pressure force on the retaining wall, kN; y_a is the height of the applied active lateral pressure force relative to the bottom of the wall, m; h_w is the depth of water next to the embankment, m; h_{cant} is the depth of the front wall cantilever, m; h_0 is the elevation of the wall above the water level, m; γ_m is the specific weight of the wall material, kN/m^3; γ_w is the specific weight of water, γ_0 is the elevation coefficient h_0 of the wall above the water level, which is assumed to be 1 kN/m^3. In formulas (1) that are used for determining width b of the wall bottom at seismic load, values E_a and y_a have to be substituted for values E_a^s and y_a^s, respectively.

When designing hydraulic structures to be erected in seismic areas, it is necessary to consider separately the seismic pressure of soil and water (in case soil is under water) on the wall during seismic impacts.

In the general case, as backfill soil is above the water level and under it, it is proposed to use the dependence for determining the ordinate e_a^s of lateral pressure of soil and water

$$e_a^s = \left(q + \gamma_w h_w + \sum \gamma_i^s y_i\right)\lambda_a^s, \quad (2)$$

where y_i^s is the resulting force of specific weight γ_i of soil and volumetric seismic force (per unit volume); h_w is the depth of water from the water table (WT) of backfill to the wall bottom; y_i is the thickness of the i-th layer of backfill soil; λ_a^s is the coefficient of active pressure (outward pressure) under seismic impact.

The value e_a^s is the ordinate of the seismic pressure diagram of soil and free water on the wall surface. The values include both soil pressure e_a^s in usual static conditions, and additional seismic pressure of soil and water on it.

The coefficient of active lateral pressure λ_a^s given angle ω of soil friction against the retaining wall under seismic impact is determined according to the dependence

$$\lambda_a^s = \frac{\cos^2(\varphi - \varepsilon)}{\left(1 + \sqrt{z}\right)^2 \cos\varepsilon}, \quad (3)$$

where

$$z = \frac{\sin(\varphi - \varepsilon)\sin(\varphi + \omega)}{\cos(\omega + \varepsilon)}. \quad (4)$$

According to the existing norms for calculating a retaining wall for seismic load [22], the most hazardous is the horizontal direction of the seismic pressure of soil. In this case

$$\gamma^s = \frac{\gamma_i}{\cos\varepsilon}, \quad (5)$$

where $\varepsilon = arctgAK_1$ is the angle of deviation from the vertical of the specific gravity equilibrium γ_i of soil and seismic force $y_i^s AK_1$, A is the coefficient whose values should be taken as equal to 0.1; 0.2; 0.4 respectively for the calculated seismic intensity of 7, 8 and 9 points, K_1 is the coefficient considering the admissible damage to buildings and structures, taken for hydraulic structures as equal to 0.25.

In the case the lateral active pressure of water-saturated soil on the retaining wall under seismic effects is determined, the weight of suspended soil y_{sb} should be introduced into the formulas, just as in case of operational load, while seismic force $y_{satur} AK_1$ should be determined according to the density of saturated soil y_{satur}. In this case, the deviation angle of the resultant is determined by the following formula

$$\varepsilon_{satur} = arctg \frac{\gamma_{satur}}{\gamma_{sb}} AK_1. \quad (6)$$

The value of the force E_a^s of the active lateral pressure on the retaining wall under seismic load is determined as the area of the active lateral pressure diagram e_a^s, and the height of application from the soil foundation is proportional to the areas of the diagram e_a^s in separate sections along the height of the retaining wall.

With a static load in formula (2), instead of the coefficient λ_a^s, the coefficient λ_a of the active lateral pressure under a static load is taken, the values of which are determined by the formula

$$\lambda_a = \left(\frac{\cos\varphi}{1 + \sin\varphi}\right)^2 = tg\left(45^\circ - \frac{\varphi}{2}\right), \quad (7)$$

where φ is calculated angle of internal friction of the backfill soil.

In this case, the force E_a of active lateral pressure under static load and the height y_a of its application relative to the ground base are calculated similarly.

Checking the stability of the retaining wall for sliding under flat shear in the plane of the sole under the action of a seismic load is performed by the formula

$$K^{plan} = \frac{N_{oper} tg\varphi + bc}{E_a^s} \geq 1.15, \quad (8)$$

where K^{plan} is the stability factor for flat shear; φ and c are respectively, the calculated angle of internal friction and adhesion of the base soil.

Checking the stability of the wall for deep shear is carried out according to the method when the slip line limiting the area of the limit state of the base soil is taken in the form of two straight segments connected to each other by a curvilinear insert described by the equation of a logarithmic spiral. The actual eccentrically loaded foundation is replaced by an equivalent centrally loaded one with a reduced width b_{red} equal to $b_{red} = b - 2e^s$, where e^s is the eccentricity of the application of the vertical force N_{oper} from the weight of the backfill wall and soil in the operational case under seismic load.

As a result, a graph of the bearing capacity of the base $\tau_{ult} = f(\sigma)$ is constructed, where τ_{ult} is the limiting shear resistance of soils. According to the voltage $\sigma_{oper} = N_{oper} / b_{red}$ in the operational case under seismic load, the corresponding limiting shear stress τ_{oper}^{ult} is determined. The safety factor for deep shear K^{deep} is finally calculated from the ratio

$$K^{deep} = \tau_{oper}^{ult} b_{red} / E_a^s \geq 1.15. \quad (9)$$

2.2. Initial parameters and loads

The calculations were carried out for a reinforced concrete retaining wall with a front cantilever. The total height of the retaining wall was 7.4 m, the water depth $h_в$ next to the embankment was 6.1 m and the height of wall elevation h_0 above water level was 1.3 m. Average sand with specific weight γ = 18.4 kN/m^3 and humidity W = 14 % was taken as backfill soil. The foundation of the retaining wall is composed of water saturated clayey soils (highly plastic clay-bearing soils) having specific weight γ = 20.0 kN/m^3 and humidity W = 24 %. The humidity of clayey soils at liquid limit W_L = 0.30 and at plastic limit W_p = 0.16. The design angle φ of internal friction of sandy soils was 32°, and that of clayey soils was 17° with cohesion c = 16.67 kPa. Elastic modulus E of sandy soils was 31 MPa and that of clayey soils was 17 MPa.

The value of the useful load q on the surface of the base (on the cordon) was 29 kPa.

Initially, the values of active lateral pressure under operational and seismic load of 7, 8 and 9 points were estimated without considering soil friction and at the angle of soil friction against the rear surface of the retaining wall being equal to the angle of internal friction of backfill soil or to its half $\varphi/2$.

For all of these cases, the width of bottom of the retaining wall was calculated.

Further comparative calculations on the bearing capacity and stability of the retaining wall were made for a maximum seismic load of 9 points without considering soil friction and at the angle of soil friction against the rear surface of the retaining wall being equal to angle φ of internal friction of backfill soil or to its half $\varphi/2$.

The results of these calculations were used for analyzing the behavior of soils under dynamic wave loads.

The calculations consider an alternative variant of the pile foundation in the base of the retaining wall. The diameter of the piles was taken as d = 30 cm depth of immersion, equal to the width of the retaining wall b.

The required number of piles is determined by a separate calculation for vertical and horizontal loads. At the first stage of the calculation, the highest of the values obtained is taken for vertical and inclined piles with the angle of installation of the piles $\alpha = 0.6\delta$, where $\delta = arctg\left(E_a / N_{oper}\right)$ or $\delta^s = arctg\left(E_a^s / N_{oper}\right)$ is the slope angle of the resultant force to the vertical for the operational (seismic) case, but no more than 19°, which corresponds to the pile slope 3:1 (given the capabilities of pile-driving equipment). The final version of the pile foundation is set by the smallest number of piles in all design cases – vertical piles or inclined piles (with the installation angle δ for an operational or seismic case).

In all cases the number of piles is maximum under the horizontal seismic load. When the piles are positioned in the plan, the distance between the axes of the piles should be at least 3D in order to maximize the bearing capacity of each pile in the cluster.

The piles must be equally loaded, for which the contact diagram σ under the bottom of the retaining wall is divided into equal areas and the axes of the longitudinal rows of piles are positioned against the centers of gravity of each of its parts.

2.3. Methodology for calculating bearing capacity and stability

In compliance with the existing norms and rules, the calculation of the retaining wall in terms of bearing capacity and stability of the bases and foundations is carried out according to group I of limit states for the main and special combination of maximum loads.

The possibility of erecting a wall on soils of a natural foundation was studied given the design pressure on the foundation. According to the existing standards, this calculation is made for two design cases when the values of maximum stresses $\sigma_{\max}$ under the bottom of the retaining wall do not exceed the limit design pressure R^p on foundation soils, as well as the average values of stresses 0.5 $\left(\sigma_{\max} + \sigma_{\min}\right)$ of value 1.2 R^p.

In addition, a computer-aided diagram of φ_c -isolines with highlighted plastic deformation zones was drawn on a personal computer using the OSNOVA-2 program developed by Prof. V.M. Kirillov. It revealed their significant distribution in the base of the retaining wall.

The presence of plastic deformation zones in the base of the retaining wall made it necessary to replace the weak foundation soils with a backfill sand cushion. In this case, the compaction of sandy backfill soils and the cushion at the base of the retaining wall must be carried out using the well-known vibrodynamic methods so that the specified soil characteristics are achieved [23, 24].

The width of the sand cushion is set equal to 0.7 of its maximum spreading depth at the right edge of the wall and its half at the left edge of the wall. In addition, the sand cushion should be re-compacted to the appropriate angle of internal soil friction in order to limit the spreading of plastic deformation zones to a depth not exceeding 0.25 b of the retaining wall width, according to the existing standards.

In case the retaining wall does not meet the shear stability condition, measures must be taken to increase the bearing capacity of the foundation. Then the retaining wall stability is calculated for the case of a sand cushion rather than weak clay soils in the foundation of the retaining wall. If a sand cushion is built in the foundation, the in-plane shear of the retaining wall may occur along a weak layer of foundation soil, and the surcharge weight G_{surch} from the sand cushion must be added to the value N_{oper} of the weight of the wall and backfill soil.

In the shear analysis of the sand cushion construction, the ultimate resistance R_{ult}^* of the foundation soils must be determined given the surcharge $q_{cant}^{found} + q_{surch}^{found}$ of the foundation uplift zones caused by the weight of the foundation soil at the depth of the retaining wall bottom and the thickness of the sand cushion. The shear resistance limit τ_{ult}^{surch} is determined by the graph $\tau_{ult} = f\left(\sigma\right)$ taking into account the increasing stresses under the bottom of the retaining wall $\sigma_{oper}^{surch} = N_{oper} + G_{surch} / b_{red}$ due to the surcharge imposed by the sand cushion layer.

The calculations have been carried out in accordance with the regulatory documents.

In general, the calculations have shown fairly similar results with and without considering the soil friction on the rear surface of the retaining wall. The results of these calculations are described in more detail below.

3. Results and Discussion

3.1. Active lateral pressure calculated for different seismic intensities

The coefficients of active lateral pressure λ_a^s calculated by formulas (3) – (6) for seismic intensity of 7, 8 and 9 points are presented in Table 1.

Table 1. The coefficients of active lateral pressure for seismic intensity of 7, 8 and 9 points.

Item No.	Angle of soil friction against the wall, ω	The coefficient of active lateral pressure of soil on the wall						
		Operational load, λ_a	Seismic intensity					
			7 points	8 points	9 points	7 points	8 points	9 points
			above water area, λ_{a1}^s			under water area, λ_{a2}^s		
1	**2**	**3**	**4**	**5**	**6**	**7**	**8**	**9**
1	0	0.307	0.321	0.336	0.365	0.336	0.365	0.431
2	$\varphi/2$	0.278	0.293	0.308	0.340	0.308	0.340	0.412
3	φ	0.277	0.293	0.311	0.347	0.311	0.347	0.434

The data in the table imply that the value of active lateral pressure coefficient λ_a under operational load is λ_a = 307 without considering the soil fraction against the wall and reduces considerably down to λ_a = 0.278(0.277) at the angle of soil friction against the wall $\varphi/2(\varphi)$.

Under seismic load of 7, 8 and 9 points in comparison with operational load, the active lateral pressure coefficient λ_a = 0.307 grows above water up to λ_{a1}^s = 0.321, λ_{a1}^s = 0.336 and λ_{a1}^s = 0.365, and under water up to λ_{a1}^s = 0.336, λ_{a1}^s = 0.365 and λ_{a1}^s = 0.431 without considering the soil friction against the wall. Under seismic load of 7 and 8 points in case the soil friction against the wall is considered, the same as under operational load, the active lateral pressure coefficient λ_{a1}^s above water reduces from λ_{a1}^s = 0.321 and λ_{a1}^s = 0.336 without considering the soil friction against the wall down to λ_{a1}^s = 0.293(0.293) and λ_{a1}^s = 0.308(0.311) at the angle of soil friction against the wall $\varphi/2$ and φ, while under water from λ_{a1}^s = 0.336 and λ_{a1}^s = 0.365 without considering the soil friction against the wall down to λ_{a1}^s = 0.308(0.311) and λ_{a1}^s = 0.340(0.347) at the angle of soil friction against the wall $\varphi/2$ and φ.

Under seismic load of 9 points, the active lateral pressure coefficient λ_{a1}^s above water reduces from λ_{a1}^s = 0.365 without considering the soil friction against the wall down to λ_{a1}^s = 0.340 and λ_{a1}^s = 0.347 at the angle of soil friction against the wall $\varphi/2$ and φ, while under water it can not only decrease from λ_{a1}^s = 0.431 without considering the soil friction against the wall down to λ_{a1}^s = 0.412 at the angle of soil friction against the wall $\varphi/2$, but also grow up to λ_{a1}^s = 0.434 at the angle of soil friction against the wall φ.

According calculations, force E_a^s of lateral active pressure on the retaining wall under seismic impact of 9 points amounts to 341.65, 357.89 and 359. 28 kN/m at the angle of soil friction against the wall $\varphi/2$, $\varphi = 0$ and φ. At the seismic intensity of 8 point, lateral active pressure force E_a^s on the retaining

wall reduces to 283.49, 304.53 and 289.05 kN/m while at seismic intensity of 7 point it decreases even further down to 257.47, 280.93 and 259.81 kN/m respectively at the angle of soil friction against the wall $\varphi/2$, $\varphi = 0$ and φ. The proportionate force E_a of lateral active pressure on the retaining wall under operating static load is 172.52, 190.56 and 171.98 kN/m.

The results of the calculations by formula (1) show that the width of the retaining wall bottom under operational load is 7.2 m without considering the friction against the rear surface of the wall. Considering the soil friction against the wall, the width of the retaining wall bottom goes down to 6.8 m for both design cases at the angle of soil friction against the wall $\varphi/2$ and φ.

The calculations by formula (1) for seismic load of 7 and 8 points show that the width of the retaining wall bottom is 8.3 and 8.6 m, respectively without considering the soil friction against the wall. Considering the soil friction against the wall, the width of the retaining wall bottom reduces from 8.3 m down to 7.9 and 8.0 m under seismic load of 7 points and from 8.6 m down to 8.3 m and 8.4 m under seismic load of 8 points, respectively at the angle of soil friction against the wall $\varphi/2$ and φ.

Similar calculations by formula (1) for seismic load of 9 points show that the width of the retaining wall bottom is 9.1 and 9.3 m respectively at the angle of soil friction against the wall $\varphi/2$ and φ, in the latter case being equal to the width of the retaining wall bottom if the calculation does not consider the soil friction against the wall.

In further calculations of the retaining wall for bearing capacity and stability, seismic intensity was assumed to be 9 points.

3.2. Results of the calculations for bearing capacity and stability

The calculations were made given the specified initial parameters for operational static load and compared to the data from previous calculations for a seismic load of 9 points without taking into account the soil friction against the retaining wall $(\varphi = 0)$.

Fig. 1 presents a common active pressure diagram drawn for the vertical plane led through the front of the retaining wall, under seismic load of 9 points.

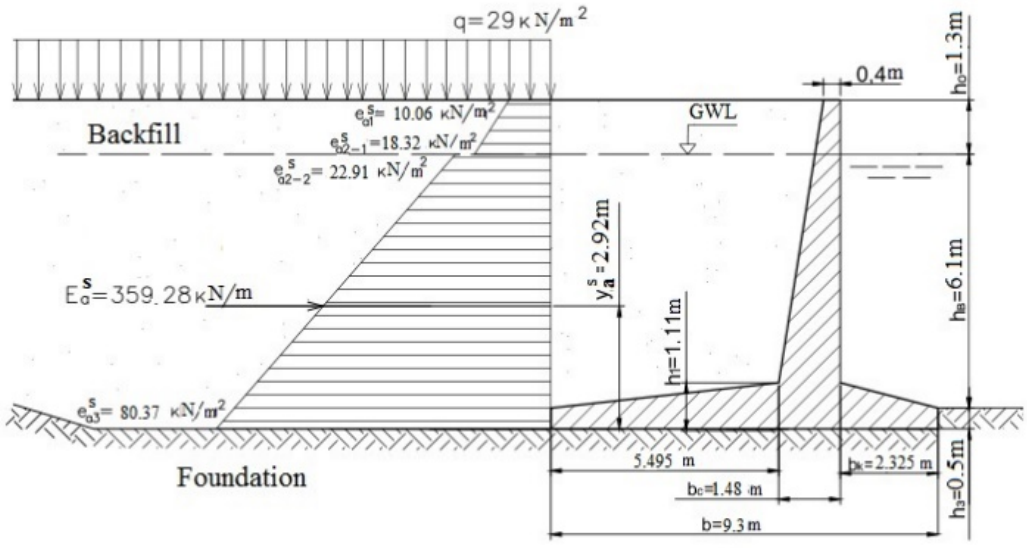

Figure 1. Diagram of active lateral pressure on a reinforced concrete corner retaining wall under seismic load of 9 points at the angle of soil friction against the rear surface $\omega = \varphi$.

The possibility of erecting a reinforced concrete corner retaining wall on natural foundation soils has been checked for construction and operational cases (under static and seismic load) by design pressure on foundation and it has been found out that the values of maximum stresses σ_{max} under the bottom of the retaining wall do not exceed the limit design pressure R^p on foundation soils or the average stress

values 0.5 $\left(\sigma_{\max}+\sigma_{\min}\right)$ of magnitude 1.2 R^{p}. Hence the design strength of foundation soils was checked and showed that a retaining wall of this type can be erected directly on natural foundation soils.

At the same time the diagram of φ_c-isolines with highlighted plastic deformation zones at the base of the retaining wall reveals that plastic deformations spread to the depth of 6.63 and 6.66 m respectively at the angle of soil friction against the wall $\varphi/2$ and φ (and $\varphi=0$).

The width of sand cushion is taken as equal to 4.64 (4/64/2 = 2.32) m at the angle of soil friction against the wall $\varphi/2$ and 4.66 (4/66/2 = 2.33) m for φ (and $\varphi=0$).

The stability of the retaining wall for in-plane shear slip under seismic load has been checked and shows that the values of stability coefficient K^{in-psb} for in-plane shear are 1.08, 1.04 and 1.05, respectively for the angle of soil friction against the wall $\varphi/2$, φ and $\varphi=0$.

The stability of the retaining wall for slip in case of in-plane shear of the bottom due to seismic load has shown that the values of the safety factor K^{in-psb} at in-plane shear do not meet the existing standards.

The calculations show that with the sand cushion layer being 2.32 (2.33) m thick, the stability coefficient rises to 1.23 for all design cases.

Fig. 2 presents a design diagram for checking the stability of a reinforced concrete corner retaining wall for in-depth shear.

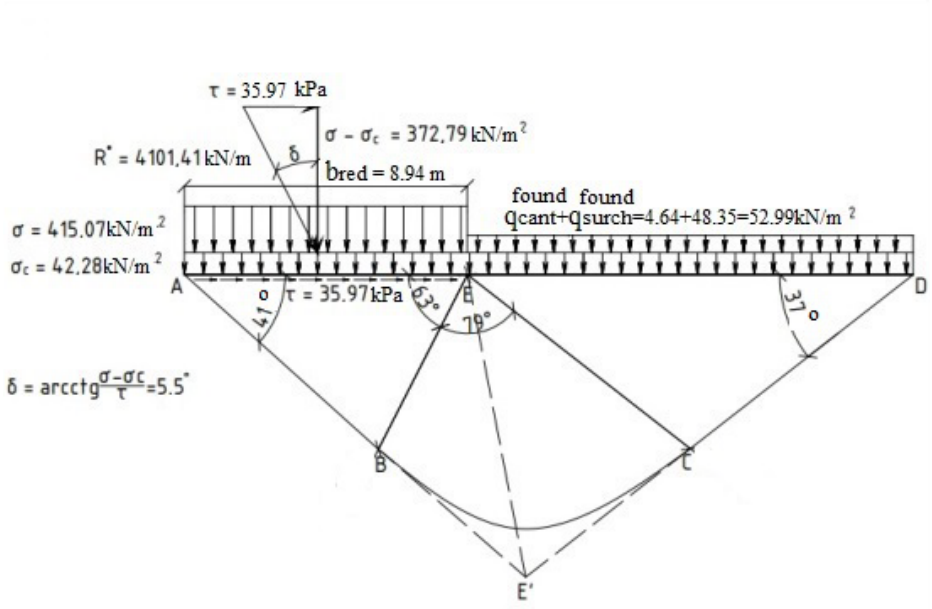

Figure 2. Design diagram for checking the stability of the retaining wall for in-depth shear at an angle of soil friction against the wall $\varphi/2$ with a sand cushion h'_n = 2.32 m thick

As a result of calculations of the retaining wall for in-depth shear, an even greater decrease in the stability coefficient K^{deep} was revealed with values of 1.02, 0.99 and 0.97 respectively at the angle of soil friction against the wall $\varphi/2$, φ and $\varphi=0$.

As a result of the calculations of the retaining wall for deep shear, a decrease in the stability margin coefficient K^{deep} is usually less than the value allowable by the existing standards.

At the same time if a sand cushion with the layer of thickness being 2.32 and 2.33 m was built, the stability coefficient could increase from 1.02 to 1.18 and from 0.99(0.97) to 1.15 respectively at the angle of soil friction against the wall $\varphi/2$ and φ (and $\varphi=0$).

Fig. 3 presents typical diagrams of foundation bearing capacity under the bottom of the retaining wall for the variant of calculation with and without surcharging the areas of soil heave provided a 2.32 m thick sand cushion is built.

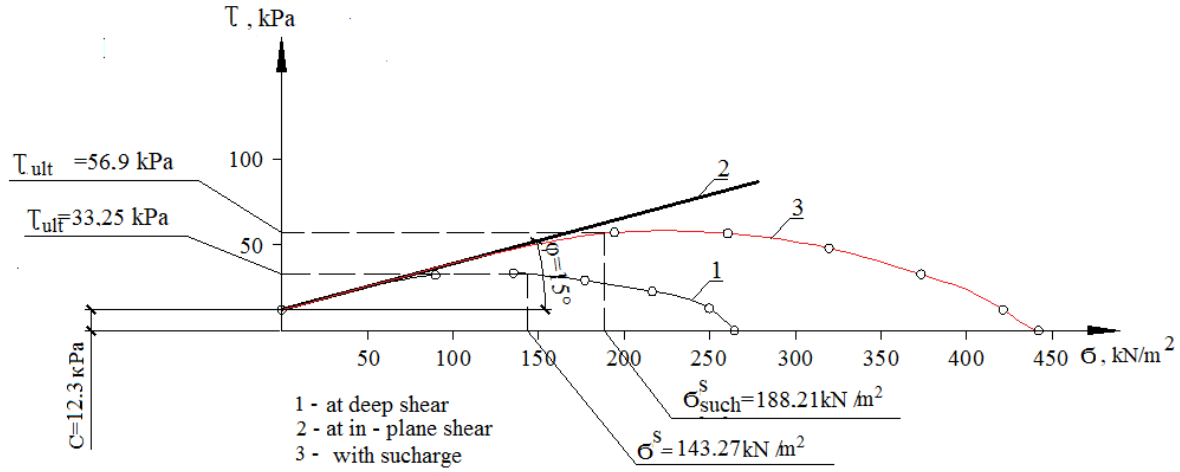

Figure 3. Graphs of the bearing capacity of the foundation of the retaining wall for in-depth shear at the angle of soil friction against the wall $\varphi/2$.

In the base of the reinforced concrete retaining wall, 81, 87 and 83 piles are required per 10 linear meters of the retaining wall, respectively, at the angle of soil friction against the wall $\varphi/2$, φ and $\varphi = 0$.

In general, similar results were obtained with and without considering the soil friction on the rear surface of the retaining wall at seismic intensity of 9 points.

3.3. Analysis of calculation results

Based on studies of soil behavior under dynamic wave loads, carried out under the guidance of Prof. P.L. Ivanova, the author of the article analyzed the results of calculations of the retaining wall, performed on the seismic load.

According to their calculations, force E_a^s of lateral active pressure on the retaining wall under seismic impact of 9 points amounts to 341.65, 357.89 and 359.28 kN/m at the angle of soil friction against the wall $\varphi/2$, $\varphi = 0$ and φ. The proportionate force E_a of lateral active pressure on the retaining wall under operating static load is 172.52, 190.56 and 171.98 kN/m. Hence, the mean value of lateral pressure e_a^{stat} at operational static load on the retaining wall is 21.84, 24.12 and 21.77 kN/m^2. Then the corresponding mean value of additional lateral pressure e_{as}^{dyn} under seismic impact on the retaining wall is 21.40, 21.18 and 23.71 kN/m^2.

This verification proves that the values of additional lateral pressure e_{as}^{dyn} under seismic impact on the retaining wall are either slightly less than the values of lateral pressure e_a^{stat} under operational static load or exceed them. This proves the fact that under seismic impact the resistance of soil fractioning against the rear surface of the retaining wall is very insignificant or absent at all.

Fig. 4 presents a typical graph of dynamic wave action on the retaining wall when the active lateral pressure force under seismic load exceeds the pressure under operational static load.

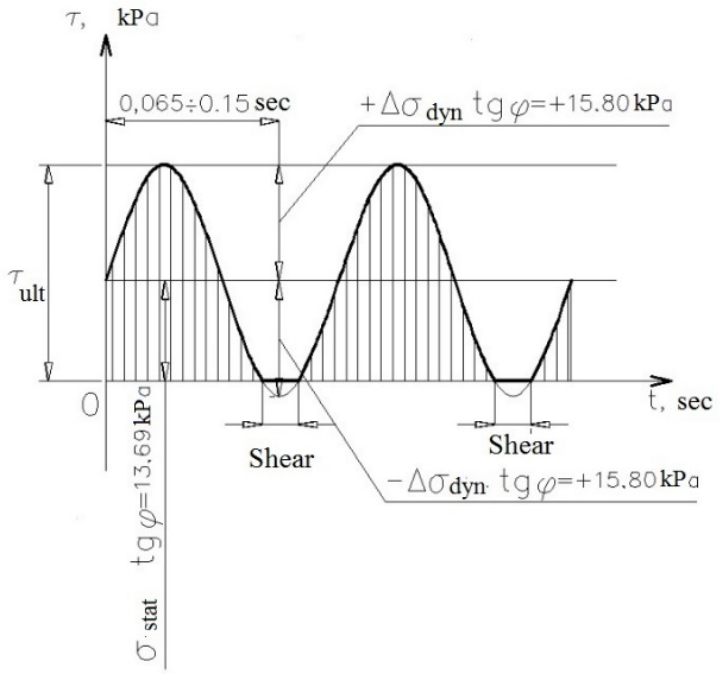

Figure 4. Graph of dynamic wave impact on the retaining wall at seismic intensity of 9 points.

In addition, at the seismic intensity of 8 point, lateral active pressure force E_a^s on the retaining wall reduces to 283.49, 304.53 and 289. 05 kN/m while at seismic intensity of 7 point it decreases even further down to 257.47, 280.93 and 259. 81 kN/m respectively at the angle of soil friction against the wall $\varphi/2$, $\varphi = 0$ and φ. Consequently, the respective mean values of additional lateral pressure e_{as}^{dyn} under seismic impact of 8 points on the retaining wall reduces to 14.05, 14.43 and 14.82 kN/m^2, while at the seismic impact of 7 point it becomes 10.75, 11.44 and 11.12 kN/m^2.

It is evident that force of lateral active pressure E_a on the retaining wall under operational static load has to be taken as earlier equal to 172.52, 190.56 and 171.98 kN/m, while the corresponding mean value of lateral pressure e_a^{stat} under operational static load on the retaining wall is 21.84, 24.12 and 21.77 kN/m^2 at the angle of soil friction against the wall $\varphi/2$, $\varphi = 0$ and φ.

Solving the inverse problem using the dependence

$$\omega = arctg \frac{\tau_{stat} - \Delta\tau_{dyn}}{\sigma_{stat}}, \tag{10}$$

where ω is the design angle of internal soil friction against the wall under dynamic action, degree; τ_{stat} is the resistance to soil friction against the wall under static action, kN/m^2; $\Delta\tau_{dyn}$ is the value of reduced resistance to soil friction against the wall under dynamic action, kN/m^2; σ_{stat} is normal stresses of lateral pressure of soil on the wall under static load, kN/m^2. It can be determined that under seismic intensity of 7 and 8 points, the angle ω of soil friction against the rear surface of the retaining wall is 0.569φ and 0.440 φ.

Fig. 5 presents a typical graph of dynamic wave action on the retaining wall when the force of active lateral pressure under seismic load does not exceed the force of active lateral pressure under operational static load.

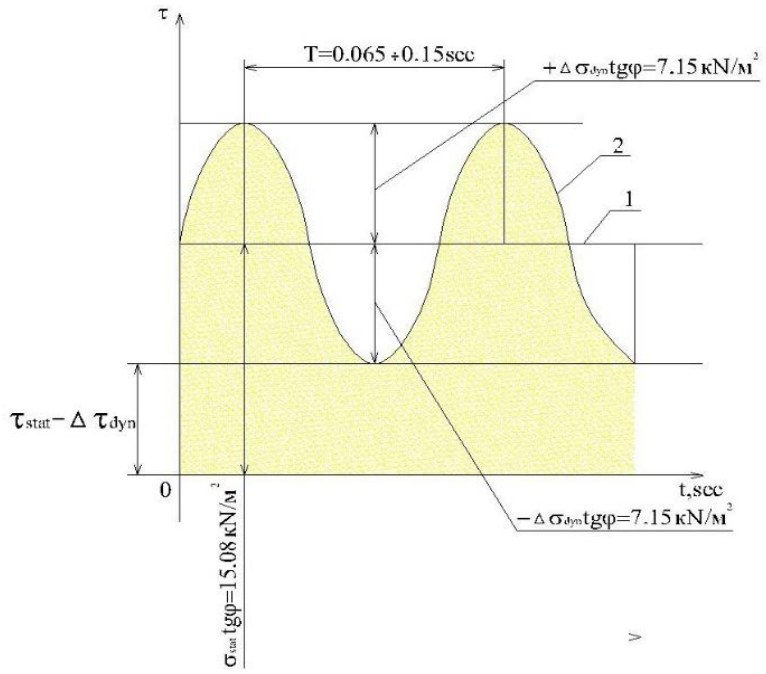

Figure 5. Graph of dynamic wave impact on the retaining wall at seismic intensity of 7 points: 1 – resistance to soil shear against the retaining wall under static load; 2 – change in resistance to soil shear under soil oscillations under seismic load.

Designations in the Figure: $\left(\tau_{stat} - \Delta\tau_{dyn}\right)$ is the least resistance to soil shear against the rear surface of the wall under dynamic (seismic) action, kN/m²; σ_{stat} is normal stresses of soil on the retaining wall under operational (static) load, kN/m²; $\pm\Delta\sigma_{dyn}$ is the change in normal stresses of soil under dynamic (seismic) action kN/m²; φ is the angle of internal friction of backfill soil, degree; T is the time of soil oscillations under seismic impact, c.

Finally transforming (10), let us write down the dependence for finding the angle ω of soil friction against the rear surface of the retaining wall at different values of the lateral soil pressure force E_a^s on the retaining wall under seismic load in the form of

$$\omega = arctg\frac{E_a - \Delta E_a^s}{E_a}tg\varphi = arctg\left(2 - \frac{E_a^s}{E_a}\right)tg\varphi, \tag{11}$$

where E_a is the force of lateral pressure of soil on the retaining wall under static load, kN; ΔE_a^s is the change in force of lateral pressure of soil on the retaining wall under seismic load; E_a^s is the maximum force of lateral pressure of soil on the retaining wall under seismic load; φ is the angle of internal friction of soil backfill.

If the value of the expression in brackets is negative, the angle ω of soil friction against the retaining wall is taken as equal to 0. In this case, under seismic impact, soil slips on the rear surface of the retaining wall.

4. Conclusion

1. At a seismic load of 9 points, the force of active lateral pressure on the retaining wall during seismic action, as a rule, exceeds the force of active lateral pressure during operational static load.

2. In this case, the calculation of the gravitational retaining wall in terms of bearing capacity and stability can be made without taking into account the friction of the soil against the retaining wall.

3. Exception the friction of the soil against the retaining wall is quite consistent with the data of Prof. Ivanova P.L. about the patterns of behavior of sandy soils under dynamic wave loads.

4. With a seismic load of 7 and 8 (or less) points, the angle of friction of the soil against the rear surface of the retaining wall should be determined from the obtained dependence (11) to determine the angle of friction of the soil under a seismic load of various intensity.

References

1. Kulmach, P.P., Filippenok, V.Z., Zaritovsky, N.G. Morskie gidrotehnicheskie soorujeniya. Chast II_ Prichalnie_ shelfovie i beregoukrepitelnie soorujeniya [Marine hydraulic structures. Part II: Berthing, shelf and shore protection structures]. Leningrad: LVVISU, 1991. 391 p.
2. Budin, A.Ya. Gorodskie i portovie naberejnie [City and port embankments]. St. Petersburg: Publishing house Polytechnic, 2014. 424 p.
3. Garibin, P.A., Belyaev, N.D. Vodnie puti i porti. Putevie raboti [Waterways and ports. Travel work]. St. Petersburg: Peter the Great SPbPU, 2014. 120 p.
4. Evtushenko, G.N., Kolosov, M.A., Silin, A.V., Narbut, R.M. Severnie porti Rossii [Northern ports of Russia]. St. Petersburg: Gidrometeoizdat Publishing House, 2006. 340 p.
5. Yakovlev P.I. Ustoichivost transportnih gidrotehnicheskih soorujenii [Stability of transport hydraulic structures]. Moscow: Transport, 1986. 191 p.
6. Bik, Yu.I., Pridanova, O.V. Snizhenie naprjazhjonno-deformirovannogo sostojanija prichal'nyh naberezhnyh s pomoshh'ju armirovanija grunta obratnoj zasypki [Reducing the stress-strain state of quayside embankments with the help of backfill soil reinforcement], River Transport (XXI century). 2009. 42 (6). Pp. 78–79.
7. Semenyuk, S.D., Kotov, Yu.N. Zhelezobetonnye podpornye stenki [Reinforced concrete retaining walls]. Bulletin of the Belarusian - Russian University. 2018. 61 (4). Pp. 86–101.
8. Lisichkin, S.E., Rubin, O.D., Atabiev, I.Zh., Melnikova, N.I. Raschjotnye issledovanija ustojchivosti i prochnosti podpornyh sten pervogo jarusa vodoprijomnika Zagorskoj GAJES [Computational studies of the stability and strength of the retaining walls of the first tier of the water intake of the Zagorskaya PSPP]. Environmental Engineering. 2012. 2. Pp. 44–48.
9. Il'ichev V.A., Mangushev R.A., Nikiforova N.S. Development of underground space in large Russan cites. Soil Mechfnics and Foundation Engineering. 2012. 49 (2). Pp. 63–67. DOI: 10.1007/s11204-012-9168-6
10. Abelev, M.Y., Averin, I.V. Determining the Deformability Characteristics of Sandy Soils at a Construction Base Using Field and Laboratory Techniques. Soil Mechfnics and Foundation Engineering. 2019. 56 (3). Pp. 164–170. DOI: 10.1007/s11204-019-09585-8
11. Shashkin, A.G., Ulitsky, V.M., Shashkin, K.G. Calculation of soil – Transport structure international. Lecture Notes in Civil Engineering. 2020. 50. Pp. 135–146.
12. Kolosov, M.A., Morgunov, K.P. The phenomena of soil liquefience in the bases of hydraulic structures. IOP Conference Series: Earth and Environmental Science. 2021. 868 (1). 012081. DOI: :10.1088/1755-1315/868/1/012081
13. Khomyakov, V., Yemenov, Y., Zhamek, N. Methods of restoration of deformed retaining walls in seismic conditions. Proceedings of 16th Asian Regional Conference on Soil Mechanics and Geotechnical Engineering, ARC 2019.Taipei, Taiwan, 2020.
14. Idriss, I.M., Boulanger, R.W. Soil liquefaction during earthquakes. EERI. USA, California, 2008. 240 p.
15. Ishihara, K., Ueno, K., Yamada, S., Yasuda, S., Yoneoka, T. Breach of a tailings dam in the 2011 earthquake in Japan. Soil Dynamics and Earthquake Engineering. 2015. 68. Pp. 3–22.
16. Towhata, I. Geotechnical Engineering Accompanied by Risk. Lecture Notes in Civil Engineering. 2021. 140. Pr. 95–109.
17. Kokusho, T. Earthquake-induced flow liquefaction in fines-containing sands under initial shear stress by lab tests and its implication in case histories. Soil Dynamics and Earthquake Engineering. 2020. 130. Pp. 121–134.
18. Zhusupbekov, A.Zh., Khomyakov, V.A., Zhagpar, A.A. Stability of hillsides at construction on sites with high seismicity. Proceedings of 14th Asian Regional Conference on Soil Mechanics and Geotechnical Engineering. Hong-Kong, China, 2011. 3. Pp. 2075–2078.
19. Stavnitser, L.R. Stability of soilbases during earthquakes Proceedings of conference on Soil Mechanics and Foundation Engineeringt. Florence, Italy, 1991. 2. Pp. 911–912.
20. Minaev, O.P. Features of calculating gravity retaining wall without assumption of base soil liquefaction. Proceedings in Earth and geosciences «Geotechnics Fundamentals and Applications in Construction: New materials, structures, technologies and calculations (GFAC 2019)». Saint Petersburg, Russia, CRC Press: Balkema the Netherlands , Taylor and Francis Group, London, 2019. 2. Pp. 182–186. DOI: 10.1201/9780429058882-35
21. Minaev, O.P. Features of calculating stability of retaining wall with significant horizontal load on base soil. Proceedings in Earth and geosciences «Geotechnics Fundamentals and Applications in Construction: New materials, structures, technologies and calculations (GFAC 2019)». Saint Petersburg, Russia, CRC Press: Balkema the Netherlands, Taylor and Francis Group, London, 2019. 2. Pp. 187–192. DOI: 10.1201/9780429058882-36
22. Stavnitser, L.R. Ceismostoikost osnovanii i fundamentov [Seismic resistance of bases and foundations]. Publishing house of the Association of Civil Engineering Universities. Moscow, 2010. 448 p.
23. Vasil'ev, Yu.S., Minaev. O.P. O vibracionnyh katkah v gidrotehnicheskom stroitel'stve. [About vibratory rollers in hydraulic engineering]. Hydraulic engineering. 2016. 2. Pp. 10–14.
24. Belash, T.A., Gorodnova, E.V., Dergachev, A.M. Ob effektivnosti uplotnenija gruntov osnovanij pri ispol'zovanii tehnologii vzryvov [On the effectiveness of soil compaction of foundations using the technology of explosions]. Natural and man-made risks. Safety of structures.2019. 6. Pp. 49–56.

Information about author:

Oleg Minaev, *PhD in Technical Sciences*
ORCID: https://orcid.org/0000-0003-0920-9081
E-mail: minaev.op@bk.ru

Received 21.12.2021. Approved after reviewing 27.04.2023. Accepted 28.04.2023.